Optimal Control of PEVs for Energy Cost Minimization and Frequency Regulation in the Smart Grid Accounting for Battery State-of-Health Degradation

Tiansong Cui[1], Yanzhi Wang[1], Shuang Chen[1], Qi Zhu[2], Shahin Nazarian[1] and Massoud Pedram[1]
[1]Department of Electrical Engineering, University of Southern California, USA
[2]Department of Electrical and Computer Engineering, University of California, Riverside, USA
{tcui, yanzhiwa, shuangc}@usc.edu, qzhu@ece.ucr.edu, {shahin, pedram}@usc.edu

ABSTRACT

Plug-in electric vehicles (PEVs) are considered the key to reducing the fossil fuel consumption and an important part of the smart grid. The plug-in electric vehicle-to-grid (V2G) technology in the smart grid infrastructure enables energy flow from PEV batteries to the power grid so that the grid stability is enhanced and the peak power demand is shaped. PEV owners will also benefit from V2G technology as they will be able to reduce energy cost through proper PEV charging and discharging scheduling. Moreover, power regulation service (RS) reserves have been playing an increasingly important role in modern power markets. It has been shown that by providing RS reserves, the power grid achieves a better match between energy supply and demand in presence of volatile and intermittent renewable energy generation. This paper addresses the problem of PEV charging under dynamic energy pricing, properly taking into account the degradation of battery state-of-health (SoH) during V2G operations as well as RS provisioning. An overall optimization throughout the whole parking period is proposed for the PEV and an adaptive control framework is presented to dynamically update the optimal charging/discharging decision at each time slot to mitigate the effect of RS tracking error. Experimental results show that the proposed optimal PEV charging algorithm minimizes the combination of electricity cost and battery aging cost in the RS provisioning power market.

1. INTRODUCTION

The increasing demands for energy resources all around the world as well as the growing public concern over the environmental effects of fossil fuels have sparked significant interests in renewable energy [1]. Plug-in electric vehicles (PEVs), which utilize electric motors for propulsion, have shown great promise in reducing the cost of transportation as well as curbing the emission due to their battery storage systems that can be flexibly recharged in a parking garage or at home [2],[3]. As more and more PEVs are being plugged into the power grid, the control or management issue of PEV charging arises, since mass unregulated charging processes of PEVs may result in degradation of power quality and damage utility equipments and customer appliances [3]. Typically, a charging aggregator is required to decide the control sequences of a group of PEVs based on technical constraints (e.g., the state-of-charge (SoC) of PEV batteries) and specific objectives (e.g., minimizing the cost of charging). The idea of coordinating PEV group charging by an aggregator has been discussed in previous works on maximizing customer convenience [4], reducing peak power demand from the grid [5], and so on.

Another promising methodology of improving power reliability is the dynamic pricing strategy in Smart Grid [6]. In the Smart Grid infrastructure, utility companies could employ real-time or time-of-use electricity pricing policies, i.e., employing different electricity prices at different time periods in a day or at different locations. This policy can incentivize consumers to perform demand side management, a.k.a. demand response, by shifting their load demands from peak hours to off-peak hours [7],[8]. As most of the vehicles are parked on average of 96% of the time [1], dynamic pricing policy offers a chance for PEV owners to reduce their electricity cost by exploiting the energy storage ability of PEV batteries through vehicle-to-grid (V2G) network [9],[10]. However, there are challenges with V2G services because it is not clear how much PEV battery aging, and therefore also the corresponding vehicle warranty, are affected by the V2G operations. Without a careful consideration of the PEV battery aging, the benefits from V2G operations can hardly be realized and widely appreciated.

Moreover, regulation service (RS) has been proved to be the most feasible service for grid-side use of PEVs in matching electricity supply with demand in real time while enabling PEV owners to reduce electricity cost by offering a reserved power capacity[11],[12]. In an RS contract, each PEV owner declares an average power consumption (for which he/she is charged) as well as a regulation service (for which he/she is credited). The vehicle is asked to modulate its power consumption dynamically through V2G network so as to track the RS signal provided by independent system operators (ISOs), who in turn try to match supply and demand in real time in presence of volatile and intermittent renewable energy generation [11]. Due to this fact, the payoff from RS provisioning should also be included in the PEV control mechanism.

To address the above-mentioned issues, we consider the problem of PEV charging under dynamic pricing and RS provisioning, with a given departure time and a given target state-of-charge (SoC) level at that time. In this problem, we explicitly take into account the degradation of battery state-of-health (SoH), which is defined as the ratio of full charge capacity of an aged battery to its designed (nominal) capacity, during V2G operations based on an accurate SoH modeling. We also consider a power market with RS provisioning, in which PEV owners are credited for the power reserves that they provide through the V2G network. The objective function to minimize therefore becomes the summation of the real energy cost during PEV charging (cost from average power consumption minus payoff from availing their power reserves) and the extra cost associated with the aging of the PEV battery. Note that it is the re-

DAC '15, June 07 - 11, 2015, San Francisco, CA, USA

http://dx.doi.org/10.1145/2744769.2744882.

sponsibility of a local controller to announce the amount of power reserves that a storage node (battery) can avail based on its current state of charge.

The rest of this paper is organized as follows. We describe the system modeling, price function, and overall cost function in Section 2. In Section 3, we provide the formulation and solution of the optimal PEV battery charging algorithm under dynamic pricing and regulations. Section 4 presents experimental results, and Section 5 concludes the paper.

2. SYSTEM MODEL

2.1 Model of PEV Storage

The most critical effect that causes power loss in the storage system of a PEV is the rate capacity effect [13]. High-peak pulsed discharging current will deplete much more of the battery's stored energy than a smooth workload with the same total energy demand. We use *discharging efficiency* of a battery to denote the ratio of the battery's output current to the degradation rate of its stored charge amount. The rate capacity effect specifies that the discharging efficiency of a battery decreases with the increase of the battery's discharging current. The energy loss in the battery during the charging process will be affected in a similar way.

Peukert's formula [14] can be used to capture the rate capacity effect. In this empirical formula, the battery charging and discharging efficiencies are described as functions of the charging current I_c and the discharging current I_d, respectively:

$$\eta_{rate,c}(I_c) = \frac{1}{(I_c/I_{ref})^{\alpha_c}},\ \eta_{rate,d}(I_d) = \frac{1}{(I_d/I_{ref})^{\alpha_d}} \quad (1)$$

where α_c and α_d are Peukert's coefficients, and their values are typically in the range of 0.1-0.3; I_{ref} denotes the reference current level for charging and discharging of the battery, which is proportional to the battery's nominal capacity C_{full}.

We call I_c/I_{ref} and I_d/I_{ref} the battery's *normalized charging current* and *normalized discharging current*, respectively. It can be observed that the efficiency values $\eta_{rate,c}(I_c)$ and $\eta_{rate,d}(I_d)$ in Eqn. (1) will be higher than 100% if the magnitude of the normalized charging or discharging current is less than one, which contradicts common sense. We therefore modify the Peukert's formula such that the efficiency values $\eta_{rate,c}(I_c)$ and $\eta_{rate,d}(I_d)$ are saturated at 100% when the magnitude of the normalized charging/discharging current is less than one, meaning that the battery suffers from no rate capacity effect for relatively low values of the charging and discharging currents.

We denote the rate of change in electric energy stored in the battery by $P_{bat,int}$, a rate which may be positive (charging the storage), negative (discharging from the storage), or zero. Based on the modified Peukert's formula, the relationship between $P_{bat,int}$ and the storage output power P_{bat} is given by

$$P_{bat} = \begin{cases} V_{bat} \cdot I_{bat,ref} \cdot (\frac{P_{bat,int}}{V_{bat} \cdot I_{bat,ref}})^{\beta_1}, & \frac{P_{bat,int}}{V_{bat} \cdot I_{bat,ref}} > 1 \\ P_{bat,int}, & -1 \le \frac{P_{bat,int}}{V_{bat} \cdot I_{bat,ref}} \le 1 \\ -V_{bat} \cdot I_{bat,ref} \cdot (\frac{|P_{bat,int}|}{V_{bat} \cdot I_{bat,ref}})^{\beta_2}, & \frac{P_{bat,int}}{V_{bat} \cdot I_{bat,ref}} < -1 \end{cases} \quad (2)$$

where V_{bat} is the battery terminal voltage and is assumed to be (nearly) constant; $I_{bat,ref}$ is the reference current of the battery storage, which is proportional to its nominal capacity C_{full} which is given in Ah (Ampere Hour); coefficient β_1 is in the range of 1.1-1.3, and coefficient β_2 is in the range of 0.8-0.9.

We use the function $P_{bat} = f_{bat}(P_{bat,int})$ to denote the relationship between P_{bat} and $P_{bat,int}$. One important observation is that this function is a convex and monotonically increasing function over the input domain $-\infty < P_{bat,int} < \infty$, as shown in Figure 1.

Due to the monotonicity property, $P_{bat,int}$ is also a monotonically increasing function of P_{bat}, denoted by $P_{bat,int} = f_{bat}^{-1}(P_{bat})$. We can see from Figure 1 that rate capacity effect makes the charging/discharging process less efficient.

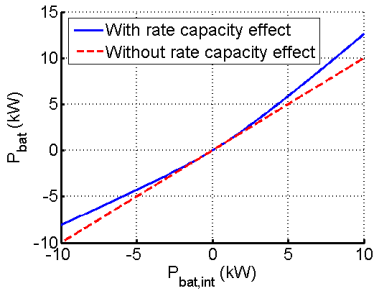

Figure 1: Relationship between P_{bat} and $P_{bat,int}$ considering the rate capacity effect.

2.2 Model of Battery SoH Degradation

State-of-health (SoH) degradation is another significant portion of power loss for PEV batteries [15]. To study the SoH degradation effect, we first formally define the state-of-charge (SoC) of a battery storage bank as follows:

$$SoC = \frac{C_{bat}}{C_{full}} \times 100\% \quad (3)$$

where C_{bat} is the amount of charge stored in the battery bank, and C_{full} is the amount of charge in the battery when it is fully charged. We interpret SoC as the state of the battery bank. On the other hand, the C_{full} value gradually decreases as a value of battery aging (i.e., SoH degradation). The amount of SoH degradation, denoted by D_{SoH}, is defined as follows:

$$D_{SoH} = \frac{C_{full}^{nom} - C_{full}}{C_{full}^{nom}} \times 100\% \quad (4)$$

where C_{full}^{nom} is nominal value of C_{full} for a fresh new battery.

The SoH of batteries is difficult to estimate because it is related to a capacity fading effect (i.e., SoH degradation) which results from long-term electrochemical reactions inside the battery. The capacity fading is related to the carrier concentration loss and internal impedance growth in the batteries. These effects strongly depend on the operating condition of the battery such as charging and discharging currents, number of charge-discharge cycles, SoC swing, average SoC, and operation temperature [16],[17]. The characterization of a battery cell requires time-consuming experiments and mathematical models are used to help us reduce the time complexity in estimating the SoH degradation. Electrochemistry-based models [18] are generally accurate but not easy to implement. Hence, we apply the SoH degradation model of Li-ion batteries proposed in [19], which can be applied to cycled charging and discharging of the battery elements and shows a good match with real data.

The SoH degradation model estimates the SoH degradation for cycled charging/discharging of a Li-ion battery cell, where a (charging/discharging) *cycle* is defined as a charging process of the battery cell from SoC_{low} to SoC_{high} and a discharging process right after it from SoC_{high} to SoC_{low}. The SoH degradation during one such cycle depends on the average SoC level SoC_{avg} and the SoC swing SoC_{swing}. We calculate SoC_{avg} and SoC_{swing} of one cycle using:

$$SoC_{avg} = (SoC_{low} + SoC_{high})/2 \quad (5)$$

$$SoC_{swing} = SoC_{high} - SoC_{low} \quad (6)$$

SoC_{swing} achieves the maximum value of 1.0 (100%) for the full 100% depth of discharge cycle, i.e., the SoC changes from 0 up to 100% and then back to 0. The SoH degradation $D_{SoH,cycle}$ during this charging/discharging cycle, accounting for both average SoC level and SoC swing, is:

$$D_1 = K_{CO} \cdot exp[(SoC_{swing} - 1) \cdot \frac{T_{ref}}{K_{ex} \cdot T_B}] + 0.2\frac{\tau}{\tau_{life}}$$
$$D_2 = D_1 \cdot exp[4K_{SoC} \cdot (SoC_{avg} - 0.5)] \cdot (1 - D_{SoH}) \quad (7)$$
$$D_{SoH,cycle} = D_2 \cdot exp[K_T \cdot (T_B - T_{ref}) \cdot \frac{T_{ref}}{T_B}]$$

where K_{co}, K_{ex}, K_{SoC}, and K_T are battery specific parameters; T_B and T_{ref} are the battery's operation temperature and reference temperature, respectively; τ is the duration of this charging/discharging cycle; τ_{life} is the calendar life of this battery. We use $D_{SoH,cycle}(SoC_{swing}, SoC_{avg})$ to denote the relationship between $D_{SoH,cycle}$, SoC_{swing}, and SoC_{avg}. The total SoH degradation (in reference to a fresh battery) after M charging and discharging cycles is calculated by:

$$D_{SoH} = \sum_{m=1}^{M} D_{SoH,cycle,m} \quad (8)$$

where $D_{SoH,cycle,m}$ denotes the SoH degradation in the m^{th} cycle.

One can observe in Eqn. (8) that the normalized SoH degradation value D_{SoH} accumulates over the battery lifetime from 0 (brand new) to 100% (no capacity left). In the literature, one typically finds values of $D_{SoH} = 20\%$ or $D_{SoH} = 30\%$, indicating 80% or 70% remaining capacity, respectively, to measure the battery's end of life. The relationship between the Li-ion battery SoH degradation versus the SoC swing and average SoC level is shown in Figure 2. In this experiment, we change the duration of a cycle to achieve different average SoC levels and SoC swings. We repeat the charge and discharge cycling until the battery reaches $D_{SoH} = 20\%$, and record the total number of cycles (i.e., the cycle life of the battery.) The results are also shown in Figure 2. There are two important observations drawn from the figure: (i) a higher SoH degradation rate is caused by both a higher SoC swing and a higher average SoC level in each charging/discharging cycle, and (ii) the cycle life of a Li-ion battery increases superlinearly with respect to the reduction of SoC swing and average SoC. We make use of these observations as well as the function $D_{SoH,cycle}(SoC_{swing}, SoC_{avg})$ in the rest of this paper.

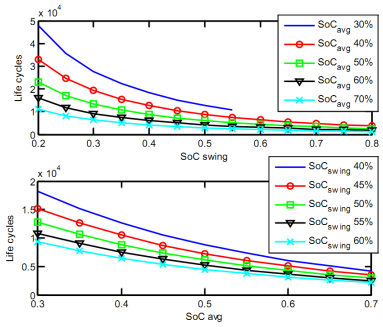

Figure 2: Li-ion battery SoH degradation versus SoC swing (at different average SoC levels) and average SoC level (at different SoC swings).

2.3 Model of Regulation Service Provisioning Market

Power market RS provisions have been widely studied in recent years [11], which are adopted to match electricity supply with demand in real time. There are several power markets with different time-scales, and we focus on the hour-ahead power market in [20] because PEVs can participate in RS provisioning market in the time scale of several hours. Currently, RS reserves are mainly offered by centralized generators. However, market rules are changing to allow the demand side, especially PEVs, to the provide reserves as well. For example, PJM, one of the largest US ISOs, has allowed electricity loads to participate in reserve transactions [21].

In this power market, each energy user declares an average energy consumption $\overline{P}$ and an RS reserve R to the power system in advance of each hour. With market clearing prices for energy consumed and RS reserves, Π^E and Π^R, the energy user is charged for its average power consumption and credited for the RS reserves such that the participant pays a net amount of $\Pi^E\overline{P} - \Pi^R R$. However, the credit for the RS reserves does not come for free. As the hour unfolds, each energy user is asked to modulate its real time power consumption $P(t)$ dynamically so as to track the RS signal $z(t)$ by ensuring that $P(t) = \overline{P} + z(t)R$ where $-1 \leq z(t) \leq 1$. It can be observed that energy users can reduce their electricity bill by providing RS reserves, while the power grid can also achieve a better match between power supply and demand in presence of volatile and intermittent renewable energy generations.

The RS provisioning market is especially promising for PEVs, because the charging policy can be expediently adjusted in order to meet the required power consumption level specified in the RS provisioning contract. When connected to the grid, each vehicle determines the optimal average power consumption $\overline{P}$ and the RS reserve R of the next time slot (hour) based on its current SoC, the target SoC, dynamic energy prices, and the credit for RS reserves. Once $\overline{P}$ and R are set, each vehicle adjusts its charging power in the next hour based on the RS signal $z(t)$ which is dynamically broadcasted from the power grid. The RS signal $z(t)$ is generated based on the real-time power market situation and is used to balance the supply and demand in the power market [22]. For each individual PEV owner who has very little effect on the entire power market, $z(t)$ can be considered as a given signal.

The uncertainty of the $z(t)$ signal complicates the optimal PEV charging schedule determination because of the following reasons: First, the PEV requires a guaranteed amount of charging energy during the parking time to satisfy a target SoC, while in the worst case, the grid might require the PEV owners to always ramp down the charging power consumption; In addition, the SoC_{swing} value has a strong dependency on the real-time charging sequence, which is directly related to the actual RS signal $z(t)$, and hence the battery SoH degradation is also dependent on the $z(t)$ signal; Finally, the SoC level of future time slots can not be accurately estimated due to the uncertainly of $z(t)$. To participate in RS provisioning market, a joint optimization framework should be developed that would consider the dynamic price of the power grid, the change of SoC_{swing} value as well as the resultant battery SoH degradation, and the uncertainty of SoC level in future time slots.

3. PROBLEM FORMULATION AND OPTIMIZATION

3.1 Problem description

In this section, we present the formulation and the solution of the cost minimization problem for a PEV in a V2G system in the context of hour-ahead power market with regulation services[1]. Assume that a PEV is scheduled to depart after N hours of parking at home or at a public parking lot, and it can thus participate in the power market for N consecutive hours. The initial SoC level of the PEV battery is given by $SoC[0] = SoC_{ini}$, and the target SoC level is SoC_{tar} when the PEV departs. We denote the dynamic energy

[1]Please note that other types of dynamic energy prices, such as day-ahead dynamic pricing, may also be supported.

price and the RS reserve revenue per unit of energy provided by the PEV during the i-th hour by $\Pi^E[i]$ and $\Pi^R[i]$, respectively, while the average power consumption and the amount of RS reserve declared by the PEV in the i-th hour are denoted by $\overline{P}[i]$ and $R[i]$, respectively. Please note that $\Pi^E[i]$ and $\Pi^R[i]$ are announced at the beginning of the i-th hour in this hour-ahead power market, and the PEV declares $\overline{P}[i]$ and $R[i]$ to the grid accordingly. During the i-th hour, the real-time power drawn from the grid can be expressed as follows

$$P(t) = \overline{P}[i] + z(t)R[i] \tag{9}$$

where $z(t)$ is the regulation signal as defined in Section 2.3.

The total cost function is comprised of two parts: the energy cost during PEV charging (cost from average power consumption minus payoff from RS reserve provisioning) and the cost associated with PEV battery aging, given as follows:

$$Cost_{total} = Cost_{energy} + Cost_{aging} \tag{10}$$

The energy cost in Eqn. (10) is calculated as follows:

$$Cost_{energy} = \sum_{i=1}^{N} (\Pi^E[i]\overline{P}[i] - \Pi^R[i]R[i]) \tag{11}$$

while the battery aging cost is given by (we assume that the battery reaches end-of-life when SoH degradation is 30%):

$$Cost_{aging} = \frac{D_{SoH}}{1 - SoH_{th}} \cdot Cost_{bat} \tag{12}$$

where $Cost_{bat}$ is the cost to purchase and replace the PEV battery, D_{SoH} represents the amount of SoH degradation during the combination of driving cycle and charging process, SoH_{th} is the threshold SoH level (typically 70%) at which the battery should be replaced.

As can be seen from Eqn. (11) and (12), $Cost_{energy}$ and $Cost_{aging}$ depend on the entire sequence of $\Pi^E[i]$ and $\Pi^R[i]$, as well as the RS signal $z(t)$ which will directly affect the battery SoC range during each hour. However, in an hour-ahead power market, one only knows the price for average power and credit for power regulation for the next hour. In order to reflect the potential opportunity for power regulation in all future hours, we propose to estimate the values of $\Pi^E[i]$'s and $\Pi^R[i]$'s based on the pricing history. Moreover, as mentioned earlier, the uncertainty of $z(t)$ adds to the difficulty of accurately calculating the total cost. To tackle this problem, rather than finding an effective approach to predict the complicated dynamics of the regulation signal, we treat $z(t)$ as a random variable that follows a specific distribution on $[-1, 1]$ which can be extracted from data in the past. Once the probability density function (PDF) of $z(t)$ is obtained, the expected behavior of the system can be estimated based on the statistics of $z(t)$.

In order to find the optimal $\bar{P}[i]$'s and $R[i]$'s to minimize the total cost of the PEV, we propose the following adaptive control framework. At the beginning of the i-th hour, $\Pi^E[i]$ and $\Pi^R[i]$ are given, and the HEV controller determines the average power consumption and the RS reserve of all future hours based on the current knowledge of the system parameters (either given or estimated). While the values of $\bar{P}[i]$ and $R[i]$ for the i-th hour are submitted to the grid, the values of $\bar{P}[i+1], \ldots, \bar{P}[N]$ and $R[i+1], \ldots, R[N]$ will be further updated at the next decision epoch at the beginning of the $(i+1)$-th hour when our knowledge of parameters including $\Pi^E[i+1]$ and $\Pi^R[i+1]$ is updated.

3.2 Adaptive Control Problem Formulation

We describe the adaptive control problem of HEV charging at the beginning of the i-th hour. At that time $\Pi^E[i]$ and $\Pi^R[i]$ are announced from the grid, and the SoC level of the HEV battery is given by $SoC[i-1]$. The amount of average power consumption and RS reserve to be submitted to the grid, i.e. $\bar{P}[i]$ and $R[i]$, are derived by HEV controller by jointly considering the next hour (the i-th hour) and all other hours in the future (the $(i+1)$-th to N-th hour). As mentioned in Section 3.1, in order to consider all future hours, the unknown parameters including the market prices, the SoC of the battery, and the SoH degradation of the battery will first be estimated. While finding these estimations, we assume that history information of the power market (e.g. pricing, regulation signal, etc.) are available.

For the market clearing price of average power consumption over hour i' $(i+1 \le i' \le N)$, $\Pi^E[i']$, we make the observation that its daily fluctuation pattern is similar across different days and a high power price in a specific hour usually implicates high prices in the following hours. Therefore, the estimated value, denoted by $\hat{\Pi}^E[i']$, is calculated as

$$\hat{\Pi}^E[i'] = \frac{\Pi^E[i]}{\bar{\Pi}^E[i]} \cdot \bar{\Pi}^E[i'] \tag{13}$$

where $\bar{\Pi}^E[i]$ and $\bar{\Pi}^E[i']$ are the average market clearing prices for average power consumption in the i-th hour and the i'-th hour in the history, respectively. In this way we effectively derive the estimation $\hat{\Pi}^E[i']$ over the i'-th hour through the given value $\Pi^E[i]$. Using the same approach, the estimated value of $\Pi^R[i']$, denoted by $\hat{\Pi}^R[i']$, can be calculated.

To estimate the SoC change and the SoH degradation of the battery of the PEV, we first extract the empirical p.d.f. (probability density function) of $z(t)$, which will be denoted by $f_Z(z)$ where $-1 \le z \le 1$. Considering the power conversion efficiency and the rate capacity effect, the relation between the power drawn from the power grid, $\bar{P}[i'] + z(t)R[i']$, and the battery charging/discharging power $P_{bat}(t)$ is given as

$$\bar{P}[i'] + z(t)R[i'] = \begin{cases} \frac{1}{\eta_C} \cdot P_{bat}(t), & P_{bat}(t) \ge 0 \\ \eta_D \cdot P_{bat}(t), & \text{otherwise} \end{cases} \tag{14}$$

where η_C and η_D are the charging and discharging efficiencies of the power converter, respectively. The relationship between $P_{bat}(t)$ and the internal input power of the battery $P_{bat,int}(t)$ is specified in Eqn. (2). Based on these two relationships we define the function $\bar{P}[i] + z(t)R[i] = f_{tran}(P_{bat,int}(t))$.

Therefore, the estimated average internal input power of the battery for the i'-th hour, denoted by $\hat{P}_{bat,int}[i']$, can be calculated as

$$\hat{P}_{bat,int}[i'] = \int_{-1}^{1} f_{tran}^{-1}(\bar{P}[i'] + zR[i'])f_Z(z)dz \tag{15}$$

And the estimated SoC values for future hours, denoted by $\hat{SoC}[i']$, are determined by:

$$\hat{SoC}[i'] = SoC[i-1] + \sum_{j=i}^{i'} \frac{\hat{P}_{bat,int}[j] \cdot \Delta_T}{V_{bat} \cdot C_{full}}, i \le i' \le N \tag{16}$$

Using functions $f_Z(\cdot)$ and $f_{tran}(\cdot)$, the approximate SoH degradation during the charging period, denoted by $\hat{D}_{SoH}$, can be calculated as follows

$$\hat{D}_{SoH} = N_C \cdot D_{SoH,cycle}(SoC_{swing}, SoC_{avg}) \tag{17}$$

where $D_{SoH,cycle}(SoC_{swing}, SoC_{avg})$ is defined as in Eqn. (7) and N_C is the equivalent charging cycles that can be calculated as

$$N_C = \frac{\Delta_T \sum_{i'} \int_{-1}^{1} \max\left(\eta_C(\bar{P}[i'] + zR[i']), 0\right) f_Z(z)dz}{2V_{bat} \cdot C_{full} \cdot SoC_{swing}} \tag{18}$$

Based on the above calculations, the adaptive control problem at the beginning of time slot i $(1 \le i \le N)$ can be formulated as follows:

Given: Current SoC level $SoC[i-1]$, target SoC level SoC_{tar}, next-hour energy pricing function $\Pi^E[i]$, RS reserve revenue $\Pi^R[i]$ and PDF of RS tracking signal $z(t)$.

Predict: Future energy pricing function and RS reserve revenue $\hat{\Pi}^E[i']$ and $\hat{\Pi}^R[i']$ for $i < i' \leq N$,

Find: SoC_{high}, SoC_{low}, $\bar{P}[i']$, and $R[i']$, for $i \leq i' \leq N$.

Minimize: Estimated Objective function in Eqn.(10)

Subject to: Charging/discharging power constraint and SoC constraint

To solve the problem efficiently after predicting the values of the unknown parameters, we propose to use a solution framework with an outer loop and a kernel algorithm. In the outer loop, we iterate over a set of possible values of SoC_{high} and SoC_{low}. In each iteration, given the range of the SoC of the battery during the charging period, we formulate an optimization problem as follows:

Find: $\bar{P}[i']$'s, $R[i']$'s, $\hat{P}_{bat,int}[i']$'s, and $\hat{SoC}[i']$'s

Minimize:

$$\Pi^E[i]\bar{P}[i] - \Pi^R[i]R[i] + \sum_{i'=i+1}^{N} (\Pi^E[i']\bar{P}[i'] - \Pi^R[i']R[i']) + \frac{\hat{D}_{SoH}}{1 - SoH_{th}} \cdot Cost_{bat} \tag{19}$$

Subject to:

$$\bar{P}[i'] + R[i'] \leq P_{max,C}, \forall i' \tag{20}$$

$$\bar{P}[i'] - R[i'] \geq P_{max,D}, \forall i' \tag{21}$$

$$\hat{P}_{bat,int}[i'] \in \left[f_{tran}^{-1}\left(-P_{max,D}\right), f_{tran}^{-1}\left(P_{max,C}\right)\right], \forall i' \tag{22}$$

$$\hat{P}_{bat,int}[i'] \leq \int_{-1}^{1} f_{tran}^{-1}(\bar{P}[i'] + zR[i'])f_Z(z)dz, \forall i' \tag{23}$$

$$\hat{SoC}[i'] = \hat{SoC}[i'-1] + \frac{\hat{P}_{bat,int}[i']\Delta_T}{V_{bat}C_{full}}, \forall i' \tag{24}$$

$$SoC[N] \geq SoC_{tar} + \sigma \tag{25}$$

$$SoC[i'-1] + \eta_C\left(\bar{P}[i'] + R[i']\right)\Delta_T \leq SoC_{high}, \forall i' \tag{26}$$

$$SoC[i'-1] + f_{tran}^{-1}\left(\bar{P}[i'] - R[i']\right)\Delta_T \geq SoC_{low}, \forall i' \tag{27}$$

$$R[i'] \geq 0, \forall i' \tag{28}$$

Constraints (20) and (21) set the bounds for the total charging and discharging power for the battery. Similarly, constraint (22) set the range for the actual energy change rate of the battery. Constraint (23) captures the relation between the input power from the grid and the energy change of the battery. Constraint (24) estimate the SoC of the battery for each future hour. Constraint (25) ensures that the SoC reaches the preset target value when the PEV departs, where σ is a parameter to account for the estimation error of the SoC, which can be set to be proportional to the average $R[i']$ values. Constraints (26) and (27) ensure that the SoC of the battery will not go beyond the SoC bound set in the outer loop with the input power modulated by the regulation signal.

Based on [23], it can be proved that $f_{trans}(\cdot)$ is a convex increasing function while $f_{trans}^{-1}(\cdot)$ is a concave increasing function. Therefore, the objective function as shown above is a convex function of all decision variables, and every inequality constraints in the formulation can be trivially transformed into a convex form. At the same time, all equality constraints are affine. Consequently, the formulated problem that is solved in each iteration of the SoC range is a standard convex optimization problem that can be solved optimally with polynomial time complexity using algorithms such as the interior point algorithm [23].

Because the kernel algorithm can be solved with polynomial time complexity and the outer loop can be achieved by a search algorithm (an exhaustive search in the worst case), the overall time complexity of the algorithm is pseudo-polynomial.

4. EXPERIMENTAL RESULTS

In the simulation, we consider an hour-ahead RS provisioning power market and the PEV is equipped with a 30kWh Li-ion battery. Two baseline solutions are used for comparison. The first baseline solution is one which constant power charging without regulation. The second baseline solution applies dynamic-pricing-aware charging control without regulation.

The charging/discharging efficiencies of the battery are set to 0.85, and the Peukert factors β_1 and β_2 are set to 1.15 and 0.87, respectively. The maximum charging and discharging power, $P_{max,C}$ and $P_{max,D}$, are set to 10kW. All SoH related parameters in Eqn. (7) are from [17], and we consider an average battery lifetime of 5 years (the normal Li-ion battery lifetime is 3-7 years) as well as a battery cost of $400. The dynamic pricing scheme for power consumption and regulation service are extracted from the locational based marginal pricing (LBMP) and regulation pricing provided by NYISO [24] for October 12th – 13th, 2014. The pricing history used for future price estimation as in Eqn. (13) is also from NYISO. At the same time, we use the sampled data by PJM [21] (sampled per 4-second interval) from May 10th, 2014 for the tracking signal $z(t)$ in our simulation. TABLE I shows the energy cost and aging cost of the optimal solution for different SoC_{ini} and SoC_{tar} values, under different total charging hours N. The energy cost and aging cost of the two baseline solutions are also shown in this table for comparison. Notice that a the energy cost might be negative, indicating that the PEV makes some profit by offering RS reservation or buying electricity when the electricity price is low while selling back when the price is high.

We first consider an extreme case that $SoC_{ini} = SoC_{tar}$, i.e., the PEV does not need to charge at all. As shown in TABLE I, our proposed solution brings an opportunity of making profit from offering RS reservation while at the same time balancing the supply and demand in the power grid (a negative energy cost is achieved). However, the revenue might not be high enough to compensate the cost of exacerbating the aging process of the battery, as the total cost is still positive.

It can be observed from TABLE I that our proposed solution achieves an total cost of 15% less than the baseline solutions on average. [2] The benefit of the proposed algorithm mainly comes from the reduction of energy cost (30% reduction on average), as PEV owners can participate in RS provisioning power market and get credit from offering RS reservation. Figure 3 shows the detailed result of our proposed optimal solution for electricity price and bidding decision under $N = 12$, $SoC_{ini} = 0.2$ and $SoC_{tar} = 0.8$. One can see that in our optimal solution, the PEV offers a considerable amount of RS reserve. The energy cost is further reduced when the total charging hours is increased. Besides the fact that longer charging time will smoothen the charging current and thus reduce rate capacity effect, our proposed solution also achieves higher profit from participating in more time slots. The adaptive solution guarantees that PEV reaches the target SoC no matter what $z(t)$ signal is broadcasted. However, longer charging time will increase the aging cost.

Another observation from TABLE I is that it is better for PEVs to start charging at a relatively low SoC_{ini} level. The reason is that under the same total charging amount, a lower SoC_{ini} will lead to a smaller SoC_{avg} and thus the aging cost can be reduced.

5. CONCLUSION

In this paper, we consider the problem of PEV charging under an hour-ahead RS reservation market with dynamic energy prices, with a given total charging time as well as a target SoC level at that time. In this problem, we explicitly take into consideration the degradation of battery SoH during V2G operations, based on an accurate SoH modeling. The total cost function therefore becomes the

[2]Please note that a pessimistic estimation of charge-discharge cycles is used in our proposed solution and the actual aging cost of our solution should be less than the presented result.

Table 1: Comparison between the Cost of Proposed Solution and Baseline Solutions

Parameters			Cost of Proposed Solution ($)			Cost of Baseline Solution 1($)			Cost of Baseline Solution 2($)		
N	SoC_{ini}	SoC_{tar}	Energy	Aging	Total	Energy	Aging	Total	Energy	Aging	Total
6	0.1	0.1	-0.01	0.61	0.60	0	0.61	0.61	0	0.34	0.34
6	0.2	0.5	0.26	0.52	0.78	0.44	0.51	0.95	0.41	0.51	0.92
6	0.2	0.8	0.60	1.06	1.66	0.98	1.04	2.02	0.91	1.04	1.95
6	0.5	0.8	0.25	1.55	1.80	0.46	1.53	1.97	0.42	1.53	1.95
8	0.2	0.5	0.23	0.63	0.86	0.40	0.62	1.02	0.35	0.62	0.97
8	0.2	0.8	0.54	1.24	1.78	0.86	1.23	2.09	0.76	1.23	1.99
8	0.5	0.8	0.22	1.88	2.10	0.40	1.87	2.27	0.45	1.87	2.22
12	0.2	0.5	0.19	0.86	1.05	0.35	0.85	1.20	0.26	0.85	1.11
12	0.2	0.8	0.45	1.63	2.08	0.70	1.62	2.32	0.60	1.62	2.22
12	0.5	0.8	0.18	2.58	2.76	0.35	2.55	2.90	0.25	2.55	2.80

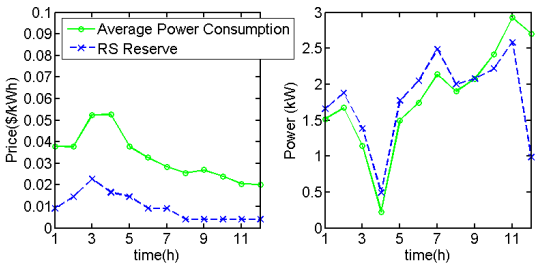

Figure 3: Electricity Price and Bidding Decision for $N = 12$, $SoC_{ini} = 0.2$ and $SoC_{tar} = 0.8$

summation of the energy cost during PEV charging (cost from declaimed average energy consumption minus payoff from declaimed RS reserves) and the extra cost associated with the aging of PEV battery. We derive an optimal control algorithm of PEV that adaptively updates its current SoC level and always makes the optimal bidding decision based on an accurately estimated price function in the future hours. The proposed algorithm also accurately accounts for the power loss during the charging and discharging process of PEV batteries, especially the rate capacity effect, and in power conversion circuits, which is often neglected in the reference work. Experimental results demonstrate that the proposed optimal PEV charging algorithm minimizes the combination of electricity cost and battery aging cost in the RS provisioning power market. We use actual data for RS reserve and dynamic energy prices and energy storage modeling from actual experiments in simulations, and the experimental result can serve practical purpose.

6. ACKNOWLEDGEMENT

This work is supported by the Software and Hardware Foundations program of the NSF's Directorate for Computer & Information Science & Engineering.

7. REFERENCES

[1] C. Chan, "An overview of electric vehicle technology," *Proceedings of the IEEE*, vol. 81, no. 9, pp. 1202–1213, Sep 1993.

[2] A. Ipakchi and F. Albuyeh, "Grid of the future," *Power and Energy Magazine, IEEE*, vol. 7, no. 2, pp. 52–62, 2009.

[3] R. Liu, L. Dow, and E. Liu, "A survey of pev impacts on electric utilities," in *Innovative Smart Grid Technologies (ISGT), 2011 IEEE PES*. IEEE, 2011, pp. 1–8.

[4] K. Shimizu, T. Masuta, Y. Ota, and A. Yokoyama, "Load frequency control in power system using vehicle-to-grid system considering the customer convenience of electric vehicles," in *Power System Technology (POWERCON), 2010 International Conference on*. IEEE, 2010, pp. 1–8.

[5] E. Sortomme and M. A. El-Sharkawi, "Optimal scheduling of vehicle-to-grid energy and ancillary services," *Smart Grid, IEEE Transactions on*, vol. 3, no. 1, pp. 351–359, 2012.

[6] R. Hassan and G. Radman, "Survey on smart grid," in *IEEE SoutheastCon 2010 (SoutheastCon), Proceedings of the*. IEEE, 2010, pp. 210–213.

[7] M. Hashmi, S. Hanninen, and K. Maki, "Survey of smart grid concepts, architectures, and technological demonstrations worldwide," in *Innovative Smart Grid Technologies (ISGT Latin America), 2011 IEEE PES Conference on*. IEEE, 2011, pp. 1–7.

[8] S. Kishore and L. V. Snyder, "Control mechanisms for residential electricity demand in smartgrids," in *Smart Grid Communications (SmartGridComm), 2010 First IEEE International Conference on*. IEEE, 2010, pp. 443–448.

[9] W. Kempton and J. Tomić, "Vehicle-to-grid power implementation: From stabilizing the grid to supporting large-scale renewable energy," *JPS*, vol. 144, no. 1, pp. 280–294, 2005.

[10] C. Guille and G. Gross, "Design of a conceptual framework for the v2g implementation," in *Energy 2030 Conference, 2008. ENERGY 2008. IEEE*. IEEE, 2008, pp. 1–3.

[11] H. Chen, C. Hankendi, M. C. Caramanis, and A. K. Coskun, "Dynamic server power capping for enabling data center participation in power markets," in *ICCAD*. IEEE Press, 2013, pp. 122–129.

[12] S. Han, S. H. Han, and K. Sezaki, "Design of an optimal aggregator for vehicle-to-grid regulation service," in *Innovative Smart Grid Technologies (ISGT), 2010*. IEEE, 2010, pp. 1–8.

[13] D. Linden and T. Reddy, "Handbook of batteries, 2002."

[14] W. Peukert, "An equation for relating capacity to discharge rate," *Electrotech, Z.*, vol. 18, p. 287, 1897.

[15] Y. Wang, X. Lin, Q. Xie, N. Chang, and M. Pedram, "Minimizing state-of-health degradation in hybrid electrical energy storage systems with arbitrary source and load profiles," in *Design, Automation and Test in Europe Conference and Exhibition (DATE), 2014*. IEEE, 2014, pp. 1–4.

[16] M. Dubarry, V. Svoboda, R. Hwu, and B. Y. Liaw, "Capacity and power fading mechanism identification from a commercial cell evaluation," *JPS*, vol. 165, no. 2, pp. 566–572, 2007.

[17] S. B. Peterson, J. Apt, and J. Whitacre, "Lithium-ion battery cell degradation resulting from realistic vehicle and vehicle-to-grid utilization," *Journal of Power Sources*, vol. 195, no. 8, pp. 2385–2392, 2010.

[18] Q. Zhang and R. E. White, "Capacity fade analysis of a lithium ion cell," *Journal of Power Sources*, vol. 179, no. 2, pp. 793–798, 2008.

[19] A. Millner, "Modeling lithium ion battery degradation in electric vehicles," in *Innovative Technologies for an Efficient and Reliable Electricity Supply (CITRES), 2010 IEEE Conference on*. IEEE, 2010, pp. 349–356.

[20] B. Kranz, R. Pike, and E. Hirst, "Integrated electricity markets in new york," *The Electricity Journal*, vol. 16, no. 2, pp. 54–65, 2003.

[21] http://www.pjm.com/.

[22] M. C. Caramanis, I. C. Paschalidis, C. G. Cassandras, E. Bilgin, and E. Ntakou, "Provision of regulation service reserves by flexible distributed loads." in *CDC*, 2012, pp. 3694–3700.

[23] S. Boyd and L. Vandenberghe, *Convex optimization*. Cambridge university press, 2009.

[24] http://www.nyiso.com/.